Journal of
Ship&Ocean
Technology
©JUNE 2004

SOTECH Vol. 8, No. 2, pp. 1~12, 2004

An Experimental Evaluation of the Coanda Jet Applied High Efficient Rudder System for VLCC

Bong-Joon Choi[1] and Hyo-Chul Kim[2]

[1] Maritime Research Institute R&D Division, Hyundai Heavy Industry, Ulsan, Korea;
E-mail: tusil39@nate.com
[2] Dept. of Naval Architecture and Ocean Engineering, Seoul National University, RIMSE, Seoul, Korea

Abstract

To keep the ocean environment from pollutions, strict international requirements on the controllability are arisen to the VLCC. Especially in low speed operations near the harbor, the VLCC is often supported by tug to replenish the insufficient rudder force.
When water jet is blown to the flapped rudder, the Coanda effect induces a high-lift force by delaying stall and re-enforcing circulation in a large angle of attack (Lachmann 1961, Ahn 2003). Based on numerous research efforts, the rudder system supported by the Coanda effect was devised and its performances were evaluated in the towing tank for a large VLCC model.
Hydrodynamic forces acting on the rudder system were measured with a water jet blowing on the rudder surface and compared with those acting on a conventional rudder. The effectiveness of the new rudder system was proven through an experimental evaluation.
Keywords: Coanda effect, Rudder performance, Circulation control, Boundary layer control, Rudder-propeller-hull interaction

1 Introduction

When a VLCC is operating at a slow speed, difficulties in providing enough maneuvering force have been frequently reported. A new rudder system supported by the Coanda effect has been devised to reinforce the conventional rudder system of a VLCC. Effectiveness of the rudder system has been proven through the various experiments in uniform flow fields.
The conventional rudder of model ship has been designed in accordance with the recommendation of DNV. This rudder system was converted into a Becker rudder system by sharing the main wing with a flap of 30% chord length to improve the performances. In this Becker rudder system, a water jet generating system was devised and accommodated in the main wing to enhance the lift force under the Coanda effect.
The hydrodynamic performances of the rudder system in uniform flow fields have been investigated experimentally by towing the rudder model in the towing tank at Seoul National University. The measured force components, themselves, clarify that the flapped rudder system could be enhanced by the Coanda effect induced in an open water condition. However, ordinarily, a rudder is installed in the disturbed wake field at rear of a ship. The

mean flow velocity at the location of the rudder is greatly retarded in the wake flow field. This speed retardation is directly related to the decrease in the rudder performances. The interaction between hull and rudder system has been evaluated by comparing the force components acting on the rudder system in a uniform flow field of an open water condition and in a disturbed flow field of behind ship condition.
In the self-propulsion condition, the mean flow velocity around the rudder system greatly increased downstream of the propeller. Because the flow velocity increased behind the propeller, the rudder performances remarkably improved. The propeller – rudder – hull interaction also was experimentally investigated at various operating conditions of the rudder. The performances of the ordinary solid rudder system and Becker rudder system with two different interlocking conditions of were measured with the three-component load cell. For the flapped rudder system, experiments were duplicated to evaluate the effect of the jet on the enhancement of the hydrodynamic force components due to the Coanda effect.
All experiments were conducted at a reduced towing speed, 0.5m/s, to emphasize the effectiveness of the Coanda rudder system when applied to the 300K VLCC at low speed operation.

2 Preparation of experimental setup

The projected lateral area of the rudder was determined in accordance with the empirical formula defined by DNV in the preliminary design stage. The detailed scale of the geometry of the rudder system was determined by referring to the lines and the stern profile of the VLCC. Especially, conveniences of the machining process of the newly devised rudder system in accommodating the Coanda jet generator within the cross section are considered in final determination of the detailed dimension. The appropriate size of the model ship was determined after that of the rudder system.

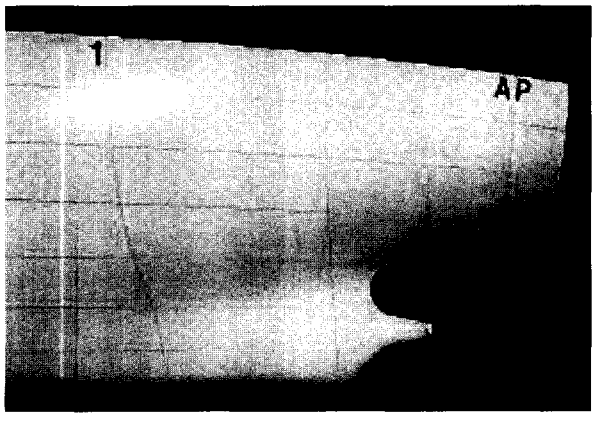

Figure 1: Stern profile of model

2.1 Model ship

For the experiment, a $1/60^{th}$ – scaled FRP model ship of 300K VLCC was prepared. This model was big enough to accommodate the measuring instruments, suitable for the free running test, even with a test pilot boarded.

Table 1: Principal particulars of the ship

	Ship	**Model**
Scale ratio	1	60
Design Speed	15 (knots)	0.9961 (m/s)
LBP (m)	320	5.3333
Breadth (m)	58	0.9667
Depth (m)	31	0.5167
Draft (m)	20.8	0.3467
LWL (m)	325.5	5.4250
WSA (m^2)	27783.6	7.7177
Volume (m^3)	314199.59	1.4546
C_B	0.814	0.814

2.2 Rudder Device

The principal dimension of the rudder system was determined, as shown in Table 2 and Figure 2, by taking account the suitable machining processes.(Kerwin et al 1972, Bamber, 1929, Abbott and von Dohenhoff 1959) The flap of the rudder system was designed to operate with the link system devised by Becker(Brix 1992). The flap angle variations were mechanically interlocked to amplify the attack angle of the main wing with the given amplification ratio. In this rudder model, the amplification ratio could be changed by simply adjusting the link mechanism. At the same time, the flap motion was linked to the saddle type prismatic cam valve so that the jet flow could be guided to only the suction side, as shown in Figure 2.(Clang 1976)

Table 2: Principal dimension of the rudder

NACA 0021	**Main Foil**	**Flap**
Chord(mm)	103	42
Span(mm)	224	224
Position of flap hinge: 24.6%c from T.E. Maximum thickness: 21%c Geometrical aspect ratio: 1.6 Rudder area: 0.0336 m^3		

Figure 2: Cross section of the designed rudder

2.3 Water Jet Injection System

Compressed air captured in the above part of the accumulation tank acts as a damper in the jet pulsation due to sudden injection. The jet injection pressure was kept constant by adjusting the pressure regulator, and the jet velocity was estimated by taking the mean of the flow rates at the nozzle section. In this system, a high pressure pump was automatically supplied the pressurized water by the pressure switch to compensate for the pressure drop.

2.4 Three-Component Load Cell

It was expected that the hydrodynamic forces acting on the rudder system would be small at low speed operation. A three-component load cell was designed to measure the rudder force, exclusively. The hydrodynamic forces transmitted to the model from the rudder could be measured in terms of the X, Y directional forces and moment acting on the Z-axis of the coordinate system of the model. The static calibration of the load cell was carried out before the main experiment was conducted. We found that the load cell had sufficient linearity, and there were negligible interferences between the force components in an arbitrary rudder angle.

3 Experiments and Results

3.1 Measurement of Open Water Characteristics of Rudder in Uniform Flow

3.1.1 Experimental Setup

The exclusively designed load cell measured the hydrodynamic force transmitted to the model when the rudder model was towed in the towing tank at the Seoul National University. The hydrodynamic lift (L), drag (D), and moment (M) acting on rudderstock were measured in accordance with the coordinate system, as shown in Figure 3. The attack angle of the rudder α is defined by the deviation angle of the main wing section from the direction of inflow. The flap angle δ is defined by the angular offset of the flap from the center plane of the main wing section.(Wilson and Von Kerczek 1979)

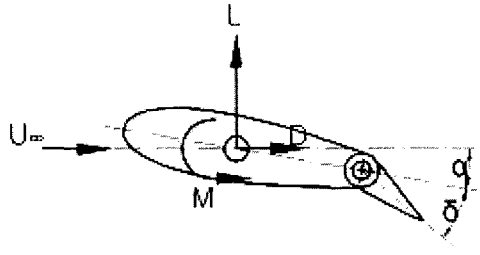

Figure 3: Force components diagram

Two different interlock conditions between wing and flap were selected, δ / α = 1/2 and 1, in the towing test of the rudder model. For each of the test condition, hydrodynamic forces were measured by varying the jet momentum coefficient. Measured forces were expressed in terms of the following dimensionless parameters:

$$C_L = \frac{L}{\frac{1}{2}\rho S U_\infty^{\ 2}} \tag{1}$$

$$C_D = \frac{D}{\frac{1}{2}\rho S U_\infty^{\ 2}} \tag{2}$$

$$C_M = \frac{M}{\frac{1}{2}\rho S c U_\infty^{\ 2}} \tag{3}$$

Where ρ is the density of the fluid (kg/m^3), S is the plane form area ($span \times chord, m^2$), c is the chord length of the rudder (m), and U_∞ is the inflow velocity (m/s). Inflow velocity was 0.5m/s and Reynolds number based on chord length of the rudder was 0.69×10^5

3.1.2 Conventional Rudder in Uniform Flow

The forces acting on the conventional rudder in uniform flow were obtained by towing the rudder model with flap locked in the neutral position. The lift force exerted by the rudder system increased linearly until the attack angle reached 15 degrees, as shown in Figure 4. Near this attack angle, a sudden drop of lift force due to the stall phenomena was observed. The hydrodynamic drag force reached minimum at the zero attack angle and increased with the increase of the attack angle. The drag force suddenly increased near the attack angle, where the stall occurred. Relatively small rudder moment was observed because of the rudderstock placed near the moment center of the wing section. The small dimension and small inflow velocity, as well as the location of the pivot center, were the reasons why the moment appeared to be negligibly small. (Hoerner and Borst 1975)

3.1.3 Effects of Flap in Uniform Flow

The hydrodynamic performances of the flapped rudder system were evaluated by the towing tests. The flap angle was interlocked with the main wing by the Becker type mechanical link system to give flap operate with amplifying the rudder motion. The experiments were carried out at two different amplifying conditions of the flap motion: δ/α = 1/2 and 1. The results are illustrated in Figure 5. The mean slope of the measured lift force of the conventional solid rudder was increased by 29% when the flap is operated with the amplification ratio δ/α = 1/2 while lift force increased by 49% when δ/α = 1. From this standpoint, the lift force, which is most important for maneuvering and controlling of a ship, could be remarkably improved by applying a flapped rudder.

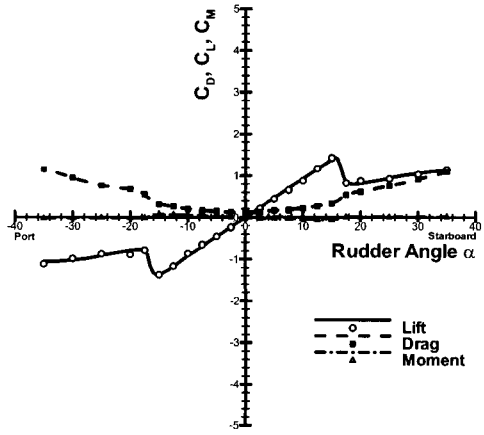

Figure 4: Performance of conventional rudder in uniform flow

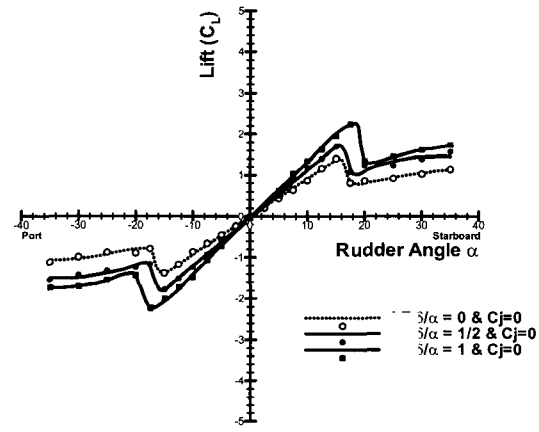

Figure 5: Hydrodynamic lift forces of Becker type flapped rudder

Table 3: Effect of flap interlock condition on increasing rate of lift curve

δ/α	Increment in slope of lift curve
1/2	**29%**
1	**49%**

3.1.4 Coanda Effects on a Flapped Rudder in Uniform Flow

To the suction side of the rudder system, a water jet was blown through the gap between the main wing and flap of the rudder. The effect of the jet flow rate was investigated by alternating the jet momentum coefficient (C_j) defined by equation (4).(Bhattacharyya 1978)

$$C_j = \frac{hV_j^2}{\frac{1}{2}cU_\infty^2} \tag{4}$$

In this equation, h is the gap width between the wing and flap (m), V_j is the velocity of the jet (m/s), c is the chord length of the rudder (m) and U_∞ is the inflow velocity (m/s).

Hydrodynamic force components acting on flapped rudder system were measured under two different amplification conditions. The ratio δ/α = 1/2 and 1 describe the flap motion. In this measurement, the rudder angle was varied from –35 degree to 35 degree and at each condition five different jet momentum coefficients C_j(0, 0.02, 0.04, 0.08, 0.16) were applied for experiments. The influences of the jet momentum coefficients on the hydrodynamic lift forces are shown in Figure 7 and Figure 8. In both cases, lift forces were increased with the increase of the flow rate. It is believed that increasing injected flow rate is effective in reinforcing the circulation around the flapped rudder system.

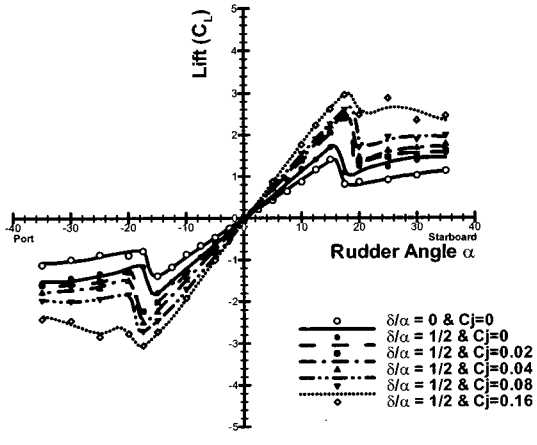

Figure 6: Effect of jet flow rate on lift ($\delta/\alpha = 1/2$)

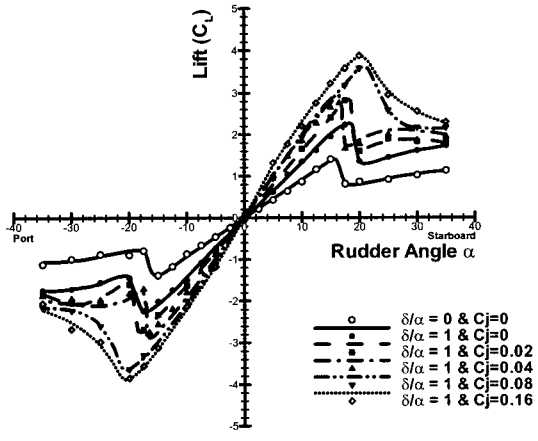

Figure 7: Effect of jet flow rate on lift ($\delta/\alpha = 1$)

The increase of lift force due to reinforcing effect of the jet blow is evident in the above figures. The data set for each test condition was line-fitted by the least square method in the region of free from stall phenomena. The slopes of lines appear to increase with the increase of the jet momentum coefficients. The slope of each line was compared with that of the conventional solid rudder. The incremental percentages increased with jet flow rate, as shown in Table 4.

Table 4: Increase of lift versus jet momentum coefficient (%)

δ/α \ C_j	**0**	**0.02**	**0.04**	**0.08**	**0.16**
1/2	**29**	**48**	**62**	**75**	98
1	49	76	96	114	138

The lift force of the conventional rudder was reinforced by 49% when the flap was controlled at the interlocking condition of δ/α=1. Additional water jet injection to this rudder system could reinforce the lift coefficient along with the increase of jet momentum coefficient (C_j). The reinforcement of the lift force recorded up to 76% when C_j= 0.02 while up to 138% when C_j= 0.16. These results imply that the low jet flow rate is sensitive in reinforcing the lift force, on the other hand, the higher jet flow rate is less sensitive in reinforcing the lift force. Thus, it is expected that the proper jet flow rate for achieving economical system efficiency can be found at the design stage.

3.2 Interaction between Rudder and Hull

3.2.1 Experimental Setup

Hydrodynamic performances of rudder model in behind ship condition were investigated as shown in Figure 8. In this experimental setup, the rudder is installed in the disturbed wake region of the model. Thus, the rudder system is exposed in the retarded flow field, and this exposure degrades the rudder performance. Such a performance change is known as the interaction between the rudder and hull.

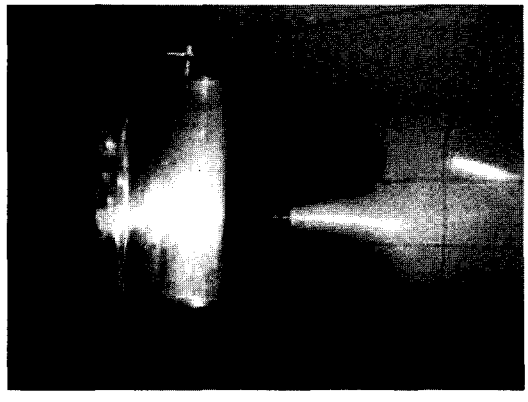

Figure 8: Rudder model in the behind ship condition

The flap operating link system was interlocked to give two different flap motion of δ/α=1/2 and 1. The experiments were carried out for various jet momentum coefficients at both interlocking conditions. The measured hydrodynamic force components were normalized by equations (1), (2), (3) by using the advancing speed of the ship U_∞. A

model test was carried out at the speed of 0.5m/s to obtain performance data of the rudder at low speed. This speed is equivalent to the Reynolds number 0.59×10^5 based on the chord length of the rudder

3.2.2 Rudder Performances in the Behind Ship Condition

The performance of the rudder in the behind ship condition was tested in the towing tank and the results were obtained as shown in Figure 9. The slopes of the performance curves were greatly mitigated when compared with Figure 4. It is believed that the retarded advancing flow velocity in the wake region generated smaller hydrodynamic forces. This may be the major reason why the hydrodynamic performance curves have mitigated the slope. It means that the mitigated performance curves should be recovered, if we use the retarded wake velocity in normalizing the measured hydrodynamic forces.

In Figure 4, stall phenomena was observed when the attack angle exceeded 15 degree, however, in Figure 9, the same stall phenomena greatly delayed to 30 degree. The major reason behind this stalling delay could be due to the effect of the retarded wake flow velocity. The slow wake velocity reduced the hydrodynamic force, and instead, the ship speed, which is greater than the wake velocity, is used in normalizing the measured hydrodynamic forces.

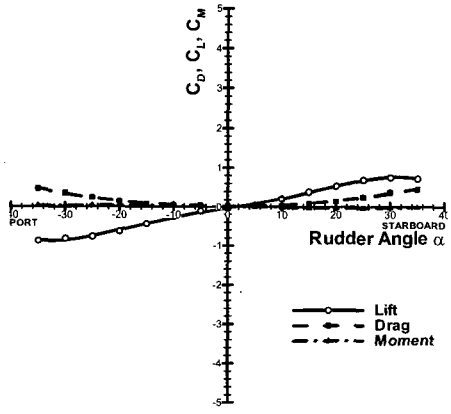

Figure 9: Performance of conventional rudder in the behind ship condition

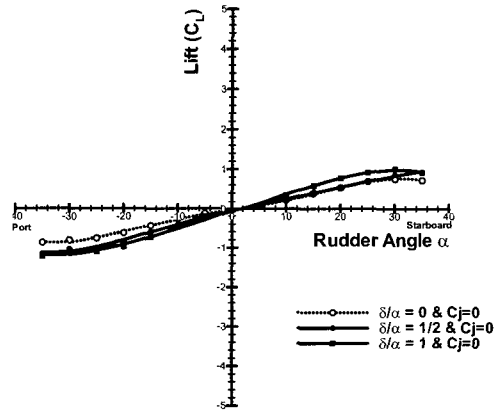

Figure 10: Performances of flapped rudder in the behind ship condition

3.2.3 Performances of Flapped Rudder in the Behind Ship Condition

The same experimental investigations on flapped rudder were carried out with interlock the link mechanism for flap control as δ/α=1/2 and 1 in the behind ship condition, as shown in Figure 10. The mean slope of the lift curve in behind ship condition appeared to have increased 27% from that of the conventional rudder when δ/α=1/2 and 63% when δ/α=1. It seems that the flapped rudder is effective even in the behind ship condition as shown in Table 5.

Table 5: Effect of flap control on increment in slope of lift curve

δ/α	Increment in slope of lift curve
1/2	**27%**
1	**63%**

3.2.4 Effects of Jet Blowing in the Behind Ship Condition

To investigate the effect of the jet injection, the hydrodynamic force components acting on flapped rudder were measured when the rudder was in the operating region of attack angle within -35~35 degree.

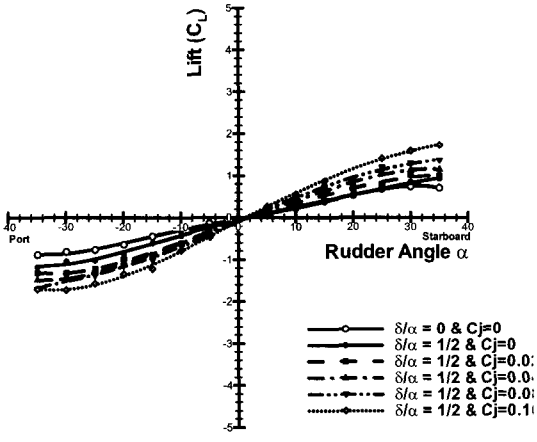

Figure 11: Effect of jet blowing on lift coefficient ($\delta/\alpha = 1/2$)

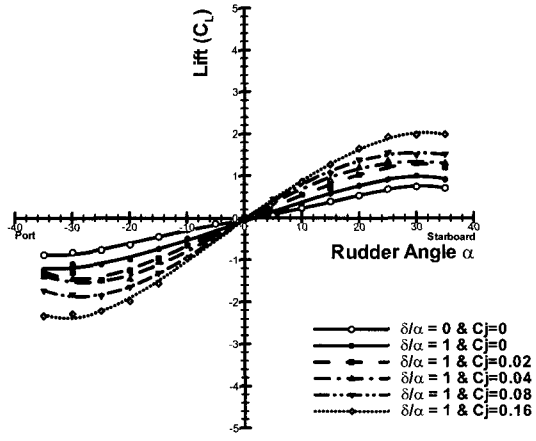

Figure 12: Effect of jet blowing on lift coefficient ($\delta/\alpha = 1$)

Two different interlock conditions, δ/α = 1/2 and 1, were selected for experimental investigation and the jet momentum coefficients, C_j (0, 0.02, 0.04, 0.08, 0.16), varied for each of the attack angles.

Figures 11 and 12 clearly show that the increase of the jet momentum coefficient is effective in reinforcing the lift force of the flapped rudder. In this behind ship condition, the reinforcing rate of the lift force from conventional rudder was greatly increased in comparison with that of the uniform flow condition, as listed in Table 6. It is believed that the retardation of the inflow velocity of the rudder in the wake region also amplifies the increase of the lift force exerted by the jet injection.

Table 6: Effect of jet injection on slope of lift curves in behind ship condition (%)

δ/α \ C_j	**0**	**0.02**	**0.04**	**0.08**	**0.16**
1/2	**27**	**79**	**97**	**119**	162
1	63	117	151	203	250

3.3 Model Ship Test in the Self-Propulsion Condition

3.3.1 Experimental Setup

Finally the performance of rudder model was evaluated in the self-propulsion condition by measuring the hydrodynamic forces components as shown in Figure 13. As a previous experiments, measuring forces acting on the rudder in the conditions of δ/α = 1/2, 1 and of various jet momentum coefficients in the downstream of propeller. Propeller rpm was adjusted to 242 rpm, which was equivalent to 0.5m/s of the self-propulsion speed. The measured hydrodynamic force components were normalized as given equations (1), (2), (3) by using the advancing speed of the ship

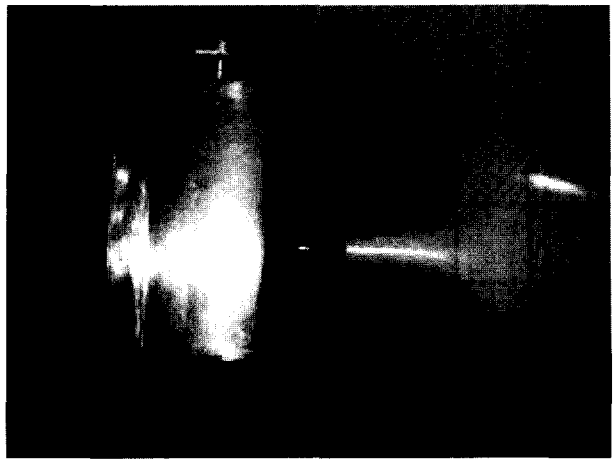

Figure 13: Model prepared for the test in self-propulsion condition

3.3.2 Performances of Conventional Rudder in the Self-Propulsion Condition

The performance of the rudder in the self-propulsion condition was markedly improved, as shown in Figure 14, because of the effect of the slipstream of the propeller.
This recovery of the hydrodynamic force, the delay of the stall, and the shift of the zero lift angle to the starboard side in the self-propulsion condition, are considered the interaction of rudder-propeller-hull.

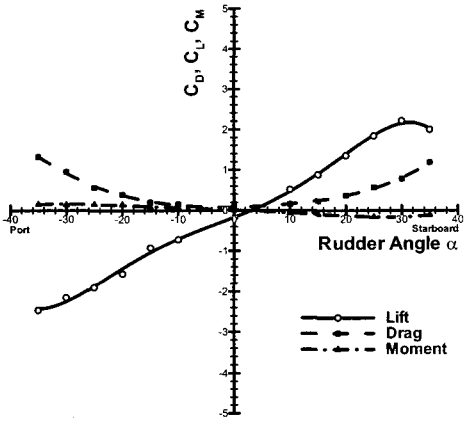

Figure 14: Conventional Rudder in the self-propulsion condition

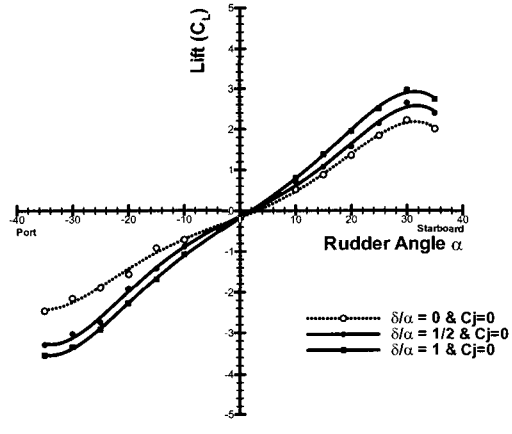

Figure 15: Flapped rudder in the self-propulsion condition

Table 7: Effect of flapped rudder on increasing rate of lift curve

δ/α	**Increment in slope of lift curve**
1/2	35%
1	64%

3.3.3 Performance of Flapped Rudder in the Self-Propulsion Condition

Figure 15 is the performance curve of the flapped rudder obtained in the self-propulsion condition. It seems that the mean slope of the measured lift force of the conventional solid rudder could be increased by 35% when the flap is operated with the amplification ratio δ/α = 1/2, and by 64% when δ/α = 1. Due to the rotating propeller slipstream, the hydrodynamic performance of the flapped rudder could overcome the drop of the performance in the ship hull wake zone.

3.3.4 Effects of Jet Blowing

As in previous tests, the flap interlocking condition, δ/α = 1/2 and 1, were adopted for the test. In this condition, the rudder angle was varied from –35 degree to 35 degree and at each condition, five different jet momentum coefficients C_j (0, 0.02, 0.04, 0.08, 0.16) were applied for experiments.

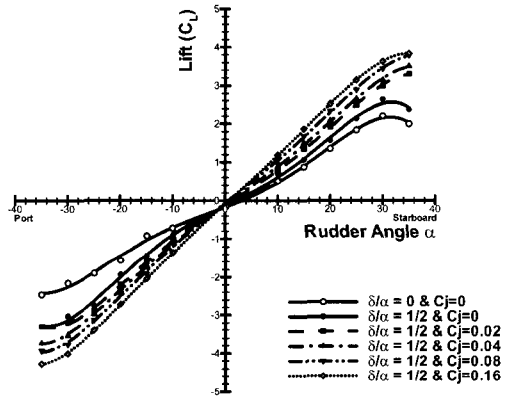

Figure 16: Effect of jet on Lift force in the self-propulsion test ($\delta/\alpha = 1/2$)

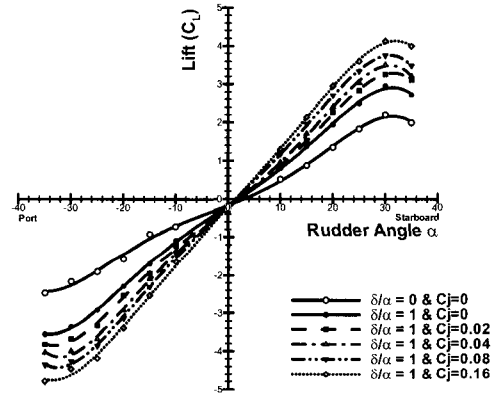

Figure 17: Effect of jet on Lift force in the self-propulsion test ($\delta/\alpha = 1$)

The influences of jet momentum coefficients on the hydrodynamic lift forces are shown in Figure 16 and Figure 17. In both cases, the lift forces were increased with the increase of the flow rate. It is believed that the increase of the injected flow rate is effective in reinforcing the circulation around the flapped rudder system.

Table 8: Effect of jet on slope of lift curves in self-propulsion condition (%)

δ/α \ C_j	**0**	**0.02**	**0.04**	**0.08**	**0.16**
1/2	**35**	**57**	**71**	**92**	114
1	64	83	102	126	153

4 Conclusions

The high-lifting rudder system was designed by utilizing the Coanda effect. The basic concept of this device is that the jet injected to the suction side of the rudder through the gap between main wing and the flap could induce the Coanda effect, which would be effective in delaying the separation phenomenon and increasing the circulation. In model

scale, the rudder system was designed and manufactured to investigate the hydrodynamic performances by towing test. The performances of the devised rudder in a uniform flow field were evaluated by a series of towing tests. The rudder in the behind ship condition was also tested to evaluate the interaction between the rudder and hull. And finally, the hydrodynamic forces transmitted to the model ship from rudderstock were investigated in a self-propulsion condition. In these series of experiments, the performances of the rudder were evaluated at various attack angles and flap angles with the jet momentum coefficients of the supplied water jet.

The experimental results obtained with 300K VLCC model test showed that the rudder device would be effective in improving the maneuvering performances of the ship. It is believed that further experimental investigation such as a turning circle test, zig-zag tests, and initial turning tests etc. should be carried out to evaluate the improvement in maneuverability of the ship.

Acknowledgements

This work was supported by the Korea Research Foundation (KRF-2002-005-D00032).

References

Abbott, I.H., A.E. Von Dohenhoff. 1959. Theory of Wing Sections. Dover Publications.

Ahn, H. 2003. An Experimental Study of the Coanda Effect on Flapped Control Surfaces. PhD. Thesis, Dept. of Naval Architecture and Ocean Eng., Seoul National Univ., Seoul, Korea

Bamber, M.J. 1929. Wind tunnel tests on airfoil boundary layer control using a backward opening slot. NACA TN No. 323

Bhattacharyya, R. 1978. Dynamics of Marine Vehicles. John Wiley & Sons Inc.

Brix, C.D.I.J. 1992. Manoeuvring Technical Manual. Seehafen Verlag

Clang, P.K. 1976. Control of Flow Separation. Hemisphere Publishing Corporation

Hoerner S.F. and H.V. Borst. 1975. Fluid Dynamic Lift. Hoerner Fluid Dynamics

Kerwin, J.E., P. Mandel and S.D. Lewis. 1972. An experimental study of a series of flapped rudder. J. of Ship Research

Lachmann, G.V. 1961. Boundary Layer and Flow Control – It's principles and application. Pergamon press

Wilson, M.B. and C. Kerczek. 1979. An inventory of some force producers for use in marine vehicle control. DTNSRDC report DTNSRDC-79/097